

Experimental Stress Analysis of Worm Wheel used in Crate Washer Gearbox

Dhairyasheel N. Powar¹, Sanjaykumar S. Gawade²

¹PG Scholar, Department of Mechanical Engineering, Rajarambapu Institute of Technology, Rajaramnagar, Urun Islampur, India.

²Professor, Department of Mechanical Engineering, Rajarambapu Institute of Technology, Rajaramnagar, Urun Islampur, India.

Abstract - The "Kolhapur Zilla Sahakari Dudh Utpadak Sangh Ltd.", Kolhapur, Maharashtra, a milk processing industry uses reduction gear box for driving conveyor belt assembly of crate washer setup used to clean the crates used for storage and transportation of milk pouches. A mentioned setup experiencing a problem of tooth failures of worm wheel used in its gear box. The motor used to drive the worm has power of 2.23 kW & speed of 1440 rpm. The speed reduction is 50:1. By studying failure pattern of damaged worm wheel teeth, excessive wear and bending fatigue are proved to be the basic reasons for gear teeth failure. The present study deals with the detailed analysis and evaluation of excessive bending stresses induced in teeth of worm gear using theoretical and experimental method. Theoretical evaluation of bending stresses in worm gears was carried out using Lewis equation and photo stress method is used for experimental stress analysis. As a result of this study, improper selection of geometrical and material parameters of worm and worm wheel for this particular application is proved to be the basic reason for failure. So, worm and worm wheel are redesigned theoretically by changing their geometrical properties and material as per required working conditions.

Key Words: Worm Gear, Bending Stresses, Reflection Polariscopes, Photo-Stress Method.

1. INTRODUCTION

Worm gear is generally used to transmit power between two non-intersecting, non-parallel shafts where high speed reduction ratio, compact drive with small overall dimensions, smooth and silent operations are required. The worm is threaded screw and worm wheel is toothed gear. In worm gears, the drive is generally given to worm. "Kolhapur Zilla Sahakari Dudh Utpadak Sangh Ltd.", Kolhapur, Maharashtra is a milk processing industry has installed the crate washer setup to clean the crates for storage and transportation of milk pouches experiencing a problem of tooth failures of worm wheel used in its gear box. Whenever worm wheel fails, it creates an unnecessary interruption in the cleaning and recurring process, which is not acceptable any more. Many reasons of worm gear failures are observed such as bending fatigue, plastic deformation, wear etc. Figure 1 shows the failure pattern of

actual damaged worm gear. By observing failure pattern of worm gear teeth, it seems that failure of worm gear is due to excessive wear and bending fatigue. Gears based on their rotational motion and the heavy amounts of load are often subjected to fatigue. Due to the application of load on the gear teeth, the gear tooth is subjected to bending.



Fig -1: Damaged worm gear

When same phenomenon is repeated for a very large number of cycles, the gear teeth fail by bending fatigue.

The bending fatigue induces in gears with formation of cracks in the root of the gear teeth which propagates with each and every rotational cycle of the gear and finally leads to the failure of gear teeth. The photo stress method gives the value of induced bending stress closely approaching to actual value [1]. The highest probability of pitting and bending failure initiation is observed in single tooth contact region due to full load sharing and the chance of contact fatigue failure is more in comparison to bending fatigue failure [2]. The basic problem of experimental strain gauge technique is the error associated with the positional accuracy of the gauge, when applied in areas of high stress gradient [3]. Errors in machining processes are responsible for high stress concentration at tooth root fillet and decrease overall life span of gear [4]. In order to study behavior of gear pairs with high value of transmission ratio, the calculation of influence variables such as mesh teeth stiffness and load distribution during mesh period should be analyzed [5]. Advanced photoelastic analysis methods used for real time monitoring of induced stress in components are less time consuming and consist of quick cure photoelastic

coatings and fringe order at any critical section can be recorded using digital camera [6]. Wear is a progressive and continuous removal of metal from the surface. Pitting is a surface fatigue failure observed in gear tooth [7].

2. THEORETICAL STRESS ANALYSIS

The worm and worm wheel used in reduction gear box is made up of EN 24 and PB₂ (Phosphor Bronze₂) material respectively. As per given data, reduction gear box of speed ratio 50:1, transmit 2.23 kW power from an electric motor (Prime Mover) to conveyor assembly of crate washer setup. Table 1 and table 2 shows the required geometrical specifications and functional parameters of worm and worm wheel required for theoretical evaluation of bending stress as,

Table -1: Geometrical Specifications of worm and worm wheel

Parameter	Worm	Worm Wheel
Pitch Circle Diameter (d_w , d_g)	22 mm	100 mm
Face Width (b)	-	26 mm
Normal Module (m_n)	2 mm	2 mm
Axial Pitch (P_x)	6.28 mm	-
No. of Starts / Teeth (Z_1 and Z_2)	1	50
Lead Angle (γ)	5.19°	-
Pressure Angle (Φ_n)	-	20°

Table -2: Functional parameters of worm and worm wheel

Parameter	Value
Permissible tangential tooth load (P_t)	15210.66 N
Torque transmitted by worm wheel (M_t)	760533.26 N-mm
Linear velocity of worm gear (V_g)	0.9765 m / s
Rotational speed of worm gear (n_g)	28 RPM
Coeff. of velocity (C_v)	0.9765
Lewis form factor (y)	0.314

Above geometrical and functional data is used to evaluate induced bending stress at the root of gear teeth is by Lewis equation (1) as,

$$\sigma_b = \frac{P_t}{C_v \cdot b \cdot \pi \cdot m_n \cdot y} \quad \dots(1)$$

Hence, as a result of above theoretical evaluation, the value of induced bending stress in worm wheel teeth was found out to be 303.66 N/mm².

3. EXPERIMENTAL STRESS ANALYSIS

In order to obtain accurate value of induced bending stress, experimental stress analysis is performed. There are numerous techniques are available such as photo stress method, stain gauge techniques, digital photography etc. Out of which Photo Stress is a widely used method used for accurate measurement of surface strains to determine the induced stresses in a test part during static or dynamic testing [4].

3.1 Significance of Photo-Stress Method

In Photo Stress method, a test surface on worm wheel is first bonded with a specially manufactured strain-sensitive plastic coating. Then, coated worm wheel is mounted on loading fixture on which the service loads of actual magnitudes are statically applied to it as per the requirements.

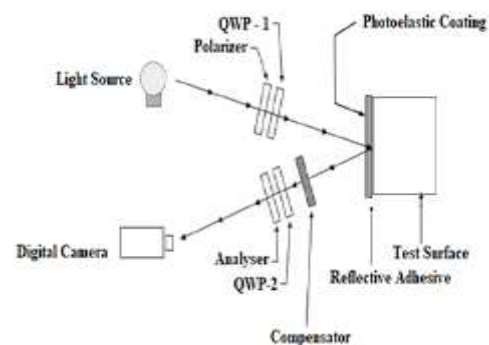


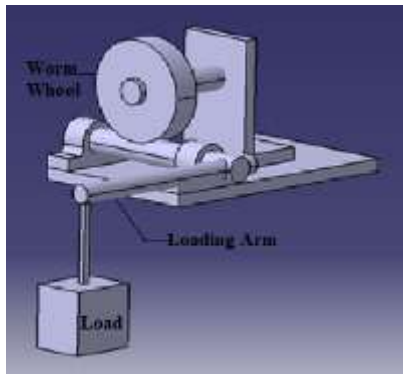
Fig -2: Schematic Representation of Reflection Polariscope

The coating is illuminated by polarized light from a reflection polariscope. When that illuminated test part is viewed through the analyser of reflection polariscope, the coated part displays the induced strains in a colorful pattern which reveals the overall strain distribution and areas with high strains. With a null balance compensator attached to the reflection polariscope setup, quantitative stress analysis can be carried out.

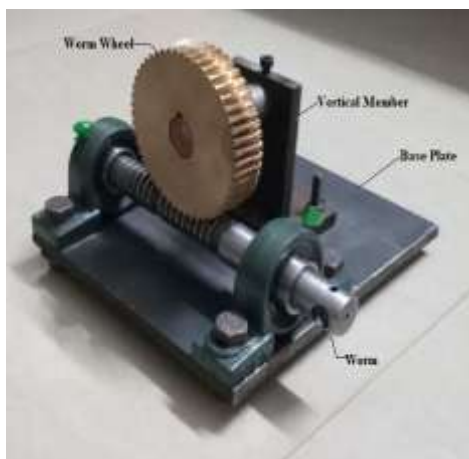
3.2 Design and Development of Experimental Setup

For more accurate evaluation of induced stresses at particular point in gear teeth, gear has to be loaded as per its service load. In order to statically simulate these actual loading conditions, special experimental setup as shown in figure 3 was designed and developed. As per actual loading

conditions, 760533.26 N-mm torque should be imparted on worm wheel teeth. Desired value of torque can be applied by providing loading arm of specified length and attaching weight at the end of loading arm. The theoretical calculations have been carried out to determine length of loading arm and weight to be attached. Finally, 70 kg weight and 1000 mm length for loading arm is selected for static simulation of actual loading conditions.



a. 3-D Model of Experimental Setup



b. Fabricated Setup

Fig-3: Experimental Setup

As shown in figure 3-a, the worm shaft is provided with lever, fitted for application of load. The worm wheel is to be located on a vertical member and its rotation is restricted. As the rotation of wheel is stopped, torque will be transferred from worm to worm wheel & stresses will be induced in worm wheel. Fig 3-b, shows the actual fabricated experimental setup.

3.3 Selection of Photoelastic Coating Materials

The selection of Photo Stress coating and their proper application on test surface is a crucial phase in Photo Stress analysis. Wide ranges of photo stress coating materials are available for application to metals. As, the coating material

should have high strain optical coefficient and sufficient thickness and the surface of gear to be coated is also flat. So, by considering above points, flat sheet of PS-1 material with 2.05 mm thickness has been selected for photo stress analysis.

3.4 Bonding of Photo Elastic Coating

Now for coating purpose, the sheet was marked as per profile of worm gear and profile is cut out by using carving machine as shown in fig.8. Roughly cut profile is then finished to match its dimensions by filing process. The surface of the worm wheel to be coated was cleaned properly. The test surface of worm wheel has been lapped lightly with abrasive paper of 120 or 220 grit as shown in fig. 4-a. Since PS-1 photo elastic sheet is used as a coating material, PC-1C adhesive was used for bonding purpose as shown in fig. 4-b. Trimmed profile of photoelastic sheet of gear's profile shape was then properly positioned and pressed down on the contacting edges with light finger pressure as shown in fig. 4-c. Finally, the coating was left to cure, for 12 hours.



a. Lapping of Gear Surface



b. Application of Adhesive



c. Bonding of Coating

Fig -4: Surface Preparation and Application of Adhesive on Gear Surface

3.5 Measurement of Fringe Order



Fig -5: Experimental Setup with loading arrangement using Reflection Polariscopes

After application of photo-stress coating on test surface of worm wheel, coated wheel along with its mating worm was mounted on experimental setup. After successful mounting of worm wheel, it is then statically subjected to loading in order to impart actual value of torque as shown in fig.5, then the resulting induced stresses causes strains over test surface.



Fig -6: Isochromatic Fringe Pattern

As coated worm wheel surface is illuminated by white light and observed through reflection polariscope, The strains developed in photoelastic coating produces proportional optical response which appear as isochromatic fringes when viewed through a reflection polariscope, isochromatic fringe patterns were observed in the coating bonded to test surface. Finally, by using photo stress plus model 832 'Null-Balance' compensator, fringe order at the root of worm wheel tooth was recorded. The isochromatic fringe patterns recorded at the root of tooth of worm wheel is as shown in fig.6.

3.6 Measurement of Bending Stress at Tooth Root

The fringe order observed in Photo-Stress coating is proportional to the difference between the principal strains or stresses in the coating or on the surface of the worm wheel. This relationship is expressed by using following equation (2) as,

$$\sigma_b = \frac{E}{1 + \mu} * \epsilon \quad \dots(2)$$

where, σ_b is the induced bending stress at the root of gear teeth, E is the modulus of elasticity of worm gear material, μ is the Poisson's ratio of worm gear material and ϵ be the principal strain developed in coating given by equation (3) as,

$$\epsilon = \frac{N_n * \lambda}{2 * k * t} \quad \dots(3)$$

Table 3 shows the required material parameters and specifications required for experimental evaluation of bending stress as,

Table -3: Parameters for Photo Stress Analysis

Parameter	Value
Recorded fringe order (N_n)	2.8
Thickness of coating sheet (t)	2.05 mm
Strain-optic coefficient (k)	0.12
Wavelength of tint of passage in white light (λ)	575 nm
Modulus of Elasticity of PB_2 Material (E)	$1.2 * 10^5$ N/mm ²
Poisson's Ratio of PB_2 Material (μ)	0.38
Principle Strain (ϵ)	$3.22 * 10^{-3}$

As a result of experimentation, fringe order recorded at root of the tooth is $N_n = 2.8$. Therefore from equation (2) and (3) induced value of bending stress at the root of the worm wheel teeth is found out to be **280.09 N/mm²**.

Table -4: Comparison of Results for existing design

Ultimate tensile strength of PB_2	Theoretically evaluated Value of induced bending stress	Experimentally evaluated Value of induced bending stress
320 N/mm ²	303.66 N/mm ²	280.09 N/mm ²

As table 4 shows, ultimate tensile strength of the PB₂ material is 320 N/mm² and values of induced bending stress obtained from theoretical and experimental stress analysis are closely approaching to the ultimate tensile strength of PB₂ material. So, factor of safety of this design is calculated as 1.05 (by referring theoretical results) which is much lesser in case of gear design. So, improper design of worm and worm wheel is the basic reason behind bending failure of worm wheel teeth. Therefore in order to reduce bending fatigue of worm wheel tooth, worm and worm wheel are need to be redesigned by changing their geometrical parameters and also to reduce surface wear, material with higher BHN value than existing PB₂ material should be selected as a base material for worm wheel.

4. REVISED DESIGN OF WORM AND WORM WHEEL

Now in revised design, higher value of module is selected, $m_n = 3$ and cast iron material is selected as base material for worm wheel, as it has higher value of hardness than existing PB₂ material and as per standard theoretical formulations, geometrical parameters of worm and worm wheel are calculated. Table 5 and 6 shows the geometrical parameters of revised design and the required functional parameters of revised worm and worm wheel design respectively.

Table -5: Geometrical Specifications of revised worm and worm wheel

Parameters	Worm	Worm Wheel
Pitch Circle Diameter (d_w, d_g)	46.62 mm	155.42 mm
Face Width (b)	-	26 mm
Normal Module (M_n)	3 mm	3 mm
Axial Pitch (p_x)	6.28 mm	-
No. of Starts (Z_1) / Teeth (Z_1 and Z_2)	1	50
Lead Angle (γ)	15.18 ⁰	-
Pressure Angle (Φ_n)	-	20 ⁰

Table -6: Functional parameters of revised worm and worm wheel

Parameter	Value
Permissible tangential tooth load (P_t)	9786.81 N
Torque transmitted by worm wheel (M_t)	760533.26 N-mm

Linear velocity of worm gear (v_g)	0.2278 m / s
Rotational speed of worm gear (N_g)	28 RPM
Coeff. of velocity (C_v)	0.9640
Lewis form factor (Y)	0.393

Above geometrical and functional data is used to evaluate induced bending stress at the root of gear teeth is by using equation (1), hence, as a result of theoretical evaluation of revised design, the value of induced bending stress in worm wheel teeth was found out to be 105.42 N/mm². As, ultimate tensile strength of the Cast Iron material is 200 N/mm², factor of safety of this design is calculated as 1.89 which is acceptable for gear design. Therefore, theoretically it can be stated that, the revised design of worm and worm wheel is safe.

In order to reduce surface wear of gear teeth, the Cast Iron material with higher value of hardness than existing PB₂ material is selected for casting the worm wheel as shown in table 7.

Table -7: Values of hardness for gear materials

Material	Hardness Value (in BHN)
PB ₂	100
Cast Iron	210

5. RESULTS & DISCUSSION

By reviewing available literature and studying different modes of gear teeth failures, it is found that excessive wear and bending fatigue are the two most common modes for gear teeth failures. Faults in design, improper selection of gear material and faulty setting up techniques are the basic causes for such type of failures. So, investigation of present work is structured accordingly. The design of gear is checked by evaluation of induced bending stress at gear teeth. This evaluation is done by two different techniques i.e. theoretical and experimental respectively for validation purpose. Photo-stress technique is used for experimentation.

In order to validate the results of theoretical stress analysis, it is required to carry out experimentation. Various techniques are available for experimental evaluation of induced stresses such as digital photography, strain gauge techniques and photo-stress techniques etc. Out of which photo-stress technique is the most suitable one for this particular case because, digital photography needs complex prerequisites and strain gauge technique is also not compatible because of smaller gear teeth dimensions. Also as per required degree of accuracy in stress evaluation is required; photo-stress technique using reflection polariscope is most suitable option. As it depends upon actual simulation of loading conditions.

As per the results obtained from Theoretical and Experimental method of stress analysis, induced values of bending stresses shown in Table 4. There is fairly good agreement between experimental and theoretical results. The percentage variation in evaluated bending stress is found to be 7.5%. So, as per the results obtained through theoretical analysis and detailed experimentations it is proved that the worm and worm wheel pair is required to be redesigned by changing geometrical parameters and base material of worm wheel. So, initial design of pair is revised by selecting higher value of module as "3" and changing worm gear material from PB₂ to cast iron as per required service conditions.

6. CONCLUSIONS

The excessive wear and bending fatigue are found out to be the two modes of gear teeth failure. The design of worm and worm wheel is evaluated by theoretical and experimental methods of stress analysis and as a result of which, factor of safety of this design is found out to be 1.05 which is much lesser. The results obtain through theoretical and experimental method of stress analysis, it can be stated that, in static state, there is fairly good agreement between experimental and theoretical results. The percentage variation in evaluated values of bending stress is found to be 7.5%.

As a result of theoretical and experimental stress analysis, improper selection of geometrical and material parameters of worm and worm wheel for this particular application is proved to be the basic reason for failure. So, worm and worm wheel are redesigned theoretically by selecting value of module as "3" as a result of which, factor of safety of this design is calculated as 1.89 which is acceptable for gear design and revised design of worm and worm wheel as per prescribed loading conditions is theoretically proved to be safe. Along with geometrical properties, improper selection of base material for worm gear is also another reason for failure. So, in order to reduce surface wear of gear teeth, material is changed from PB₂ to cast iron which has higher value of surface hardness. As per the results of theoretical analysis of revised pair it can be stated that the values of induced bending stresses in gear teeth can be minimised by selecting higher values of normal module and as values of normal modules increases, tangential load acting on worm gear teeth reduces accordingly.

REFERENCES

1. Prashant Jaysing Patil, Maharudra S. Patil and Krishnakumar D. Joshi. "Dynamic State or Whole Field Analysis of Helical Gear." *Journal of The Institution of Engineers (India): Series C* (2017): pp.1-6.
2. Paras Kumar, Harish Hirani and Atul Agrawal. "Fatigue failure prediction in spur gear pair using AGMA approach." *Materials Today: Proceedings Vol.4* (2017): pp. 2470-2477.
3. Timothy J. Lisle, Brian A. Shaw and Robert C. Frazer. "External spur gear root bending stress: A comparison of ISO 6336:2006, AGMA 2101-D04, finite element analysis and strain gauge techniques." *Mechanism and Machine Theory Vol. 111* (2015): pp. 1-9.
4. B. Kozłowska. "Two-dimensional experimental elastic-plastic strain and stress analysis." *Journal of Theoretical and Applied Mechanics Vol. 52* (2013): pp. 419 – 430.
5. Ivana Atanasovska, Marija Vukšić Popović and Zorica Starčević. "The dynamic behaviour of gears with high transmission ratio." *International Journal for Traffic and Transport Engineering Vol. 2* (2012): pp.153 – 160.
6. G. Calvert, J. Lesniak, M. Honlet. "Applications of modern automated photoelasticity to industrial problems." *Real Time Stress Monit. Vol 44* (2002): pp. 224-227.
7. P.J.L. Fernandes. "Tooth Bending Fatigue Failures in Gear." *Engineering Failure Analysis Vol. 3* (1996): pp. 219-225.